Wave propagation in mechanical metamaterials

Zhou, Y.; Zhou Y.

Chapter 1

Introduction

People conventionally use simple mechanical properties to classify states of matters: a solid maintains both fixed volume and shape, a liquid maintains a fixed volume but has a variable shape, and a gas has both variable volume and shape [1]. In recent years, new forms of matter called mechanical metamaterials appeared with unique properties [2–14]. Such metamaterials are artificial structures with effective mechanical properties that qualitatively differ from those of their base materials. An example from this thesis is the mechanical kagome lattice model shown in Fig. 1.1. This model has a free mechanism for deformation so that it does not maintain either shape or volume. This is a mechanical property that is independent of the LEGO base materials of solid plastics.

Structure determines properties [15]. The structure of mechanical metamaterials begins with repeating unit cells as building blocks. Each unit cell can be regarded as a tiny mechanical device transforming input forces and motions into a designed set of output forces and motions. The unit cells are connected to each other, forming a whole piece of material. In this way, the inputs and outputs of the unit cells are synthesized into an ordered pattern, which is just the macroscopic response of a metamaterial to a given macroscopic input. This macroscopic response can be described by linear waves [16, 17], solitary waves [18–20], or non-wavelike mechanical motions [4, 5, 9, 21]. Theoretical understanding of this physical process is indispensable for designing the structures and controlling the properties of metamaterials.

(a) **(b)**

Figure 1.1. Model of a mechanical metamaterial: twisted kagome lattice. As all the small triangles twist together, the whole structure in (**a**) contracts to the one in (**b**).

Mechanical metamaterials can affect the propagation of linear sound waves. Such acoustic metamaterials (c.f., electromagnetic metamaterials) can display special properties such as negative refractive indices that provide functionalities in acoustic cloaking devices [16, 22, 23]. In contrast with these linear-wave-based metamaterials, one can also consider mechanical metamaterials that involve large nonlinear deformations [1]. When mechanical stimuli are applied to the materials, their building blocks can display motions of rotation, twist, etc., with large amplitudes, which lead to significant changes of shape and volume of the whole system. This behavior of "large responses for small perturbations" is a key feature of *soft matter* [24].

In the past few years, the concept of topological phases was introduced into the field of mechanical metamaterials, leading to the so-called *topological mechanical metamaterials* [25, 26]. This concept not only merges the features of both acoustic waves and large deformations into one system, but also creates a link between the study of mechanical metamaterials and modern condensed matter physics. This thesis will explore the interplay between nonlinearities and the topological properties of mechanical metamaterials. First, we explain the topological phases in the next section.

[1] Sometimes they are simply referred to as *mechanical metamaterials* in a narrower sense, as opposed to acoustic metamaterials. In this thesis, we use the broader definition.

1.1 Topological mechanical metamaterials

We focus on the topological rotor chain as an example of topological mechanical metamaterials [2]. It is a chain of classical rotors connected by springs (see Fig. 1.2). The angles θ_n of the rotors are measured in an alternating fashion along the lattice, from the negative y-axis at odd-numbered sites and positive y-axis at even-numbered sites. The equilibrium angle $\overline{\theta}$ for a uniform lattice configuration can be either positive or negative, corresponding to two equilibrium states: all rotors leaning either to the right or to the left. We impose periodic boundary conditions, so the system is forbidden to switch from one equilibrium state to the other without deforming springs. In equilibrium states, all springs are at their rest length $\overline{\ell}$. When linear mechanical waves propagate in the chain, the angles θ_n oscillates around equilibrium. This causes spring deformations $\delta\ell_n$ that are determined by the displacements of the rotor angles $\delta\theta_n$. We will focus on $\delta\theta_n$ and $\delta\ell_n$ to demonstrate the idea of topological mechanics.

(a) $\overline{\theta} > 0$, right-leaning rotors **(b)** $\overline{\theta} < 0$, left-leaning rotors

Figure 1.2. Topological rotor chains with (**a**) positive and (**b**) negative equilibrium angles $\overline{\theta}$. The masses (blue dots) of rotors (black rods) rotate around fixed pivots (black crosses) and are connected to each other by springs (red dashed lines). The lattice spacing is a, the rotor length is r, and the spring equilibrium length is $\overline{\ell}$. Periodic boundary conditions are used, indicated by dangling springs at chain ends.

Because the rotors are in a one-dimensional lattice, their linear motion can be described by lattice waves. The normal modes representing a $\delta\theta$ wave

[2] B. G. Chen pointed out that a topological mechanism (essentially a rotor chain with pinning points displaced) was in one of Leonardo da Vinci's notebooks. See Ref. [27], particularly Fig. 5.

and a $\delta\ell$ wave with angular frequency ω and wave vector k are

$$\delta\theta(n,t) \propto \exp\left[i(kna - \omega t)\right], \tag{1.1}$$
$$\delta\ell(n,t) \propto \exp\left[i(kna - \omega t + \phi(k))\right] \tag{1.2}$$

where n is the nth rotor or spring along the chain, a is the lattice spacing, t is time, and $\phi(k)$ is a phase difference between a $\delta\theta$ wave and its corresponding $\delta\ell$ wave. ϕ is a crucial to the concept of topological mechanics, we will focus on it shortly after. Note that the lattice waves with wave vector k and $k + 2\pi/a$ are equivalent, because the physical quantities like $\delta\theta$ and $\delta\ell$ take values only at lattice points na, and $e^{i(2\pi/a)na} = e^{i2\pi n} = 1$.

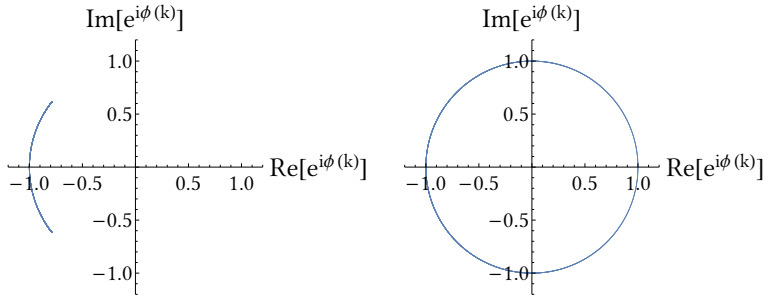

(a) $\overline{\theta} > 0$, right-leaning rotors **(b)** $\overline{\theta} < 0$, left-leaning rotors

Figure 1.3. Contour plot in the complex plane of $e^{i\phi(k)}$ for complete circuit of k from $k = 0$ to $k = 2\pi/a$. In (**a**), $e^{i\phi(k)}$ goes back and forth on the arc and indeed forms a closed loop.

As long as $\delta\theta$ and $\delta\ell$ do not vanish, the quotient $\delta\ell(k)/\delta\theta(k) \propto e^{i\phi(k)}$ is a non-zero complex number. When we tune the wave vector from $k = 0$ to $k = 2\pi/a$, in other words when we gradually decrease the wavelength from infinity to a (see Fig. 1.5 and Fig. 1.6), the phase shift between $\delta\theta$ and $\delta\ell$ waves $e^{i\phi(k)}$ runs through a closed loop on the complex plane (see Fig. 1.3). The number of times this loop turns around the origin is a *topological index*, and it has been shown [18, 25, 26] that this index is either 0 or 1, depending on which equilibrium state the chain is in (see also Eq. (1.4)). In other words, the phase of a $\delta\ell$ wave shifts by either *zero* (Fig. 1.5) or *one* (Fig. 1.6) more period

than its corresponding $\delta\theta$ wave. The correspondence between $\delta\ell$ and $\delta\theta$ as follows: we regard the $\delta\theta$ wave as $\exp[ikna]$ spatially and the $\delta\ell$ wave as $\exp[ik(na+\phi/k)]$, i.e., the effect of the phase ϕ on the $\delta\ell$ wave is a positional shift of the $\delta\theta$ wave in real space. As we will discuss later, it is the *difference* between the topological indices of the two equilibrium states of a rotor chain that make it a model of a topological mechanical material. Note that Eq. (1.1) and (1.2) make an arbitrary choice that $\delta\ell$ waves have the phase shift ϕ. We can also have $\delta\theta$ take the extra phase shift, and the reasoning remains the same.

In Fig. 1.5 and Fig. 1.6, we focus on spatial periods at $n = 0$ by thick colored lines, in order to eliminate the direct contribution of k to the phases and single out the effect of $\phi(k)$. The number of periods of extra wave shifts of $\delta\ell$ is the topological invariant.

The physical reason for this extra phase shift ϕ is the following: the deformation $\delta\ell(n,t)$ of a spring depends *asymmetrically* on the angular displacement of its two neighbor rotors, say $\delta\theta(n,t)$ and $\delta\theta(n+1,t)$. Indeed at linear order

$$\delta\ell(n,t) = -b\delta\theta(n,t) + c\delta\theta(n+1,t) \tag{1.3}$$

where b and c are prefactors that are not equal for rotor chains with $\overline{\theta} \neq 0$. Combining this equation and Eq. (1.1) and (1.2), $\delta\ell$ waves can be expressed

$$\delta\ell(n,t) \propto (c\exp[ika] - b)\delta\theta(n,t). \tag{1.4}$$

We see that the complex term $(c\exp[ika] - b)$ is the origin of the phase difference between $\delta\theta$ and $\delta\phi$ waves. This term's complex argument is just $\phi(k)$. It has been shown that the two states of right-leaning and left-leaning rotors have their b and c's values exchanged [18, 25, 26, 28]. The topological indices are defined only when $b \neq c$, i.e., the deformation depends asymmetrically on the displacements. When $b = c$, then the complex term goes to zero at $k = 0$, so the phase $\phi(k = 0)$ is not well defined, which in turn means the topological index is not well defined either [3]. The system corresponds to

[3]This is why a gapped band structure where this complex term never equals zero is necessary for a system to be "topological".

$\overline{\theta} = 0$, which is clearly symmetrical, meaning that the rotors are vertically up and down alternatively, leaning towards neither the left nor the right.

As mentioned in Ref. [25], topological indices depend on how the labels of rotors and springs are assigned. Our assignment shown in Fig. 1.5 and Fig. 1.6 produces topological indices 0 (right-leaning) and 1 (left-leaning). Other assignments may give different results. For instance, with the assignment that the nth spring connecting the $(n+1)$th and $(n+2)$th rotors (see Fig. 1.4), the same chain has topological indices 1 (right-leaning) and 2 (left-leaning). This is intuitive, since the right-leaning state and the left-leaning state are mirror symmetrical, so they cannot have intrinsic *a priori* preference in topological indices. While the topological indices depend on arbitrary choices, their differences, for example at an interface, have a well-defined physical meaning.

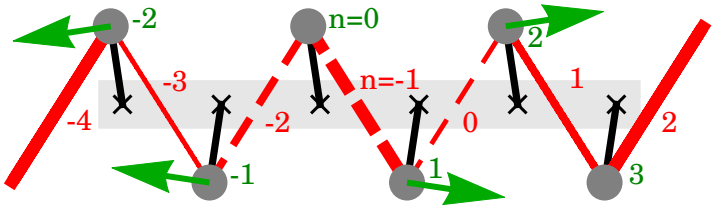

Figure 1.4. The same chain as in Fig. 1.6 but with the assignment of the nth spring connecting the $(n+1)$th and $(n+2)$th rotors. It has a topological index 2.

In the above example, the rotor chain with periodic boundary conditions is forbidden to go from one equilibrium state to the other without deforming springs. Strictly speaking, in such a case, the aforementioned assignments of labels of rotors and springs lack global consistency, because it is not possible to know whether the assignments are the same for the two states when one state cannot be *continuously* translated into the other. In other words, we have to make two assignments separately for the two states and cannot guarantee that they are consistent with each other. To avoid this, we can consider a system with positive energy so that finite spring deformation is allowed. We can also use free boundary conditions so that the two equilibrium states can be transformed into each other via zero-energy nonlinear waves, as we will see in Chapter 2. Alternatively, we can have a system with two or multiple

states put together with interfaces. In any such cases, we are able to make the assignment only once so that it is guaranteed to be consistent for all different states. Then the use of topological indices is rigorously valid.

Since Kane and Lubensky [25] introduced the concept of "band topology" into classical mechanical systems, the research of topological mechanical metamaterials has become a booming field. Many models have been proposed [13, 14, 17–19, 26, 28–46], and a universal classification of topological phonons has been provided [47]. One can map quantum mechanical problems to classical mechanics, and using spring extensions and mass displacements is not the only way of introducing topology into mechanical system. Still, we hope that the interpretation of topological phase shift in rotor chains given in this section will provide guidance in investigating wave propagation in topological mechanical systems.

This thesis will focus on linear and nonlinear propagation of waves and their interaction with impurities in mechanical metamaterials. In the next section, we present the outline of this thesis.

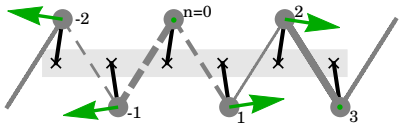

(a) $\delta\theta_n$ for $k = \frac{\pi}{3a}$, rotors right-leaning.

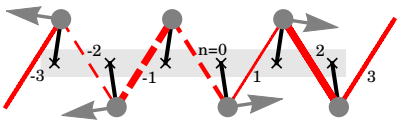

(b) $\delta\ell_n$ for $k = \frac{\pi}{3a}$, rotors right-leaning.

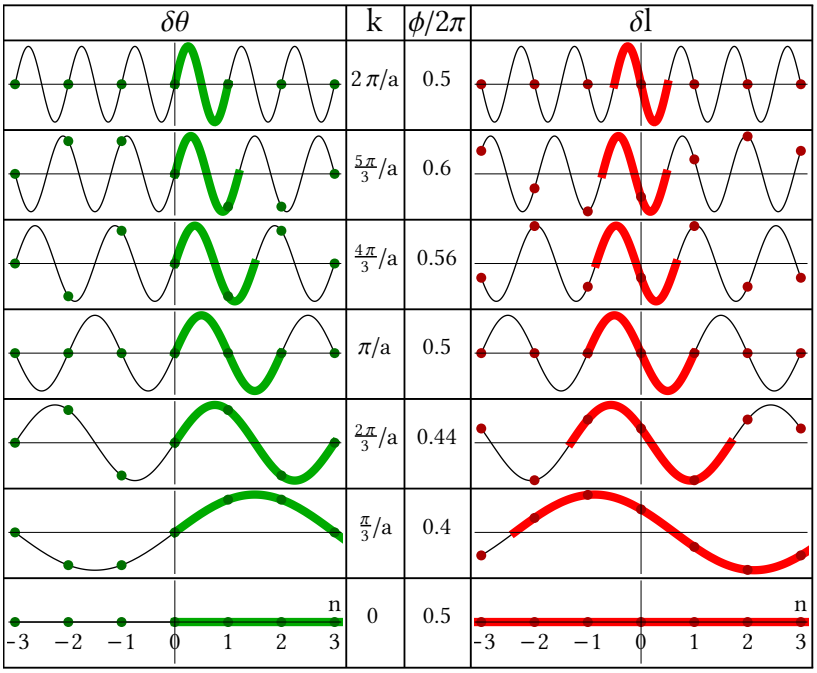

(c) Comparison of phases of $\delta\theta$ and $\delta\ell$ waves in real space with varying k.

Figure 1.5. Topological phases of a rotor chain's vibrational waves. In the configuration (**a**) and (**b**), the arrows indicate directions and amplitudes of rotor vibrations, i.e., $\delta\theta$ lattice waves, and the lines connecting rotors indicate spring deformations, i.e., $\delta\ell$ lattice waves. Dashed springs are stretched and solid springs are compressed, with their thickness proportional to deformation. In (**c**), the dots are wave values at lattice points, i.e., $\delta\theta_n$ and $\delta\ell_n$. One spatial period in the $\delta\theta$ wave and its counterpart in the $\delta\ell$ wave is emphasized by thick colored lines. The $\delta\ell$ wave stays around the same place in real space after k goes from 0 to $2\pi/a$. So the topological index of this chain with right-leaning rotors is zero. The geometrical parameters are $r/a = 0.8$ and $\bar{\theta} = +0.15$, i.e., the rotors are right-leaning.

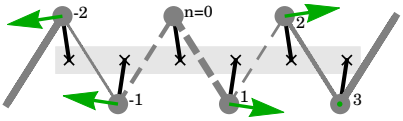

(a) $\delta\theta_n$ for $k = \frac{\pi}{3a}$, rotors left-leaning.

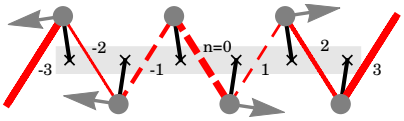

(b) $\delta\ell_n$ for $k = \frac{\pi}{3a}$, rotors left-leaning.

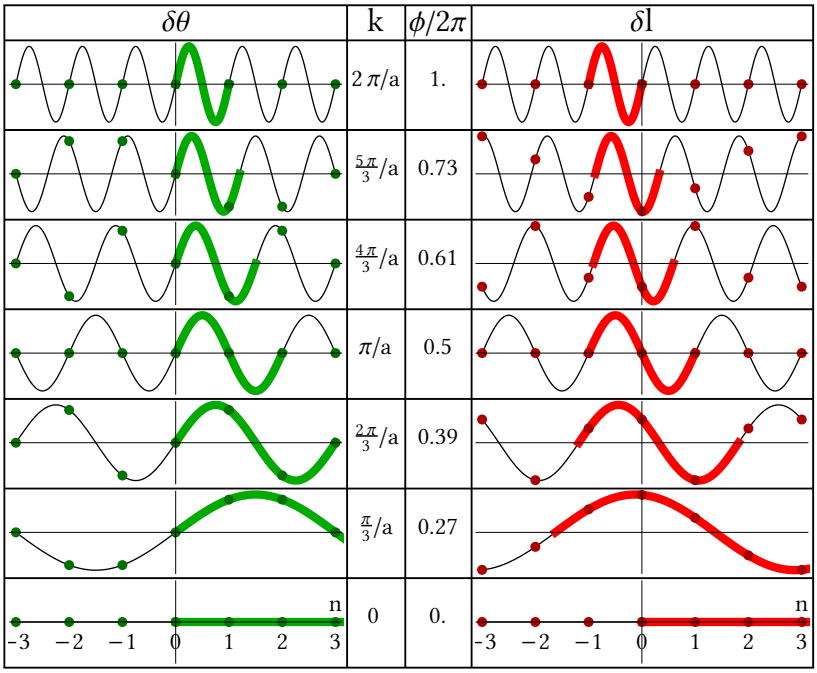

(c) Comparison of phases of $\delta\theta$ and $\delta\ell$ waves in real space with varying k.

Figure 1.6. The same setup as Fig. 1.5 except for a negative $\overline{\theta} = -0.15$, i.e., the rotors are left-leaning. The $\delta\ell$ wave drifts leftward by one period in real space after the wave vector k goes from 0 to $2\pi/a$. Thus the topological index of this chain is one.

1.2 Outline of this thesis

In mechanical metamaterials, large deformations can occur in systems which are topological from the point of view of linear waves. The interplay between such nonlinearities and topology affects wave propagation. Beyond perfectly periodic systems, defects provide a way to modify and control the properties of metamaterials, and can also interact with both nonlinearities and the bulk topology [48, 49].

While the Kane-Lubensky rotor chain (see Sec. 1.1) is an archetypal topological mechanical metamaterial, the kink and antikink solitons in the nonlinear Klein-Gordon equation are archetypal examples of nonlinear behavior [50–52]. In Chapter 2, we study the full nonlinear dynamics of this rotor chain. In the continuum description, we derive a nonlinear field theory which admits topological kinks and antikinks as nonlinear excitations. A topological boundary term, however, breaks the symmetry between the two and favors the kink configuration. Using a cobweb plot, we develop a fixed-point analysis for the kink motion and demonstrate that kinks propagate without the Peierls-Nabarro potential energy barrier typically associated with lattice models. Using continuum elasticity theory, we trace the absence of the Peierls-Nabarro barrier for the kink motion to the topological boundary term which ensures that only the kink configuration, and not the antikink, costs zero potential energy. Further, we study the eigenmodes around the kink and antikink configurations using a tangent stiffness matrix approach appropriate for pre-stressed structures to explicitly show how the usual energy degeneracy between the two no longer holds. In Chapter 3 , we show how the kink-antikink asymmetry also manifests in the way these nonlinear excitations interact with impurities introduced in the chain as disorder in the spring stiffness. Then we discuss the effect of impurities in the spring length and build prototypes based on simple linkages that verify our predictions.

To investigate similar nonlinear behavior in higher spatial dimensions, we first need a detailed understanding at the linear level (where interesting features already occur). Deformed kagome lattices are known to exhibit topological phases [13, 25], and as we shall see, may possess configurations where nonlinear effects cannot be ignored. In Chapter 4, we examine the linear mechanical waves in twisted kagome lattices, which are deformed from

the standard kagome lattice by a zero-energy twisting mechanism. In the perfect lattices, we find that this twisting mechanism tunes the phonon band structure by opening a band gap. At a critical twisting angle, we observe a surprising two-fold degeneracy of the phonon bands, which seems to be related to bonds becoming orthogonal. In Chapter 5, we introduce point defects into the lattices. Defect modes, which are spatially localized and spectrally isolated, appear in the band gap. We show that the hybridization of defect modes can be described by tight-binding models.

When the kagome lattice is untwisted (Fig. 1.1a), there are entire lines of aligned bonds which lead to zero modes at linear level [53]. Similarly, when the kagome lattice is twisted at the critical angle (Fig. 1.1b), neighboring bonds become orthogonal, and the phonon spectrum is two-fold degenerate. In both cases, such properties are related to a decoupling between some degrees of freedom which only occurs at the linear level, and we expect nonlinearities to change the picture. To prepare for a full nonlinear analysis of the kagome lattices, we first focus on a simpler one-dimensional model which should reproduce some of their key features. In Chapter 6, we investigate the propagation of nonlinear transverse elastic waves induced by a point impact of constant velocity in a tension-free flexible string. Transverse waves on a tension-free string have vanishing velocity up to linear order. Waves in the longitudinal and transverse directions are decoupled at linear level but become coupled at the nonlinear level. Even though they become shock waves when the string is under impact, they can be understood from the perspective of linear transverse waves riding on the tensioned region behind longitudinal wave fronts induced by the impact.